Materials Horizons

ROYAL SOCIETY OF CHEMISTRY

COMMUNICATION

View Article Online
View Journal | View Issue

Check for updates

Cite this: *Mater. Horiz.*, 2020, 7, 1387

Received 12th September 2019,
Accepted 23rd January 2020

DOI: 10.1039/c9mh01448a

rsc.li/materials-horizons

A nature-inspired protective coating on soft/wet biomaterials for SEM by aerobic oxidation of polyphenols†

Hong Key Park, [a] Daiheon Lee, [a] Haeshin Lee *[a] and Seonki Hong *[b]

Phenolamine networks are one of the major structural components in the insect exoskeletons called cuticles. An insect cuticle-inspired surface protective coating named "aerobic oxidation of polyphenol leading to artificial exoskeleton", APPLE, is reported. The coating layer can be formed on any solid surface, because the oxygen in the air triggers the formation of the APPLE coating. The oxidized pyrogallol, called pyrogallol-quinone, is rapidly reacted with polyamine to form mechanically robust organic thin film networks. As some insect cuticles can be directly imaged under extreme conditions, such as in the vacuum chamber of a scanning electron microscope (SEM) without conventional metal deposition, the surface morphology of APPLE-coated materials (particularly soft ones) can also be imaged by SEM without conventional metal deposition. The APPLE coating is a pure organic flexible layer which is formed within a couple of minutes. Another advantage of the APPLE layer is the suppression of the vapor gas emission from the soft materials, allowing SEM imaging of wet samples such as hydrogels and living tissues. Considering that the traditional studies of phenolic molecules focus mostly on surface functionalization, our study opens a new research direction in which such phenolic coatings might be useful for applications in extreme conditions.

New concepts

A wet sample must be fixed, dehydrated, and metal sputtered to make it amenable for SEM imaging. These conventional preparation steps provide biased images and are laborious. We report an alternative wet/soft sample preparation method for SEM analysis using an organic coating, which occurs in an interface-specific manner utilizing air O_2. Rapid couplings between phenolic molecule, pyrogallol (PG), and poly(ethylenimine) (PEI) are triggered by O_2 in ambient air, allowing it to be used on any wet or dry solid substrate as long as the samples are exposed to air. In particular, we discovered that PG/PEI coating prevents dehydration and local electron charging, demonstrating that it is useful for wet sample imaging. Other properties of the coating include shape retention and thermal protection. The phenol-amine coating chemistry is similar to sclerotization (*i.e.* skin tanning) in insects, mimicking the robust protecting functions of the insect body.

Introduction

A stiff and hard material known as a cuticle covers the whole body of an insect, functioning as an exoskeleton with soft tissues located inside. In contrast, vertebrate bones, to which soft tissues are attached, perform endoskeletal functions. The cuticle is directly exposed to external environments, acting as a protective layer. Some insects, for example, the African chironomid *Polypedilum vanderplanki* larvae, survive at temperatures as low as −270 °C and as high as 100 °C.[1] Additionally, this species can survive without a water supply for several days[2] and under gamma rays or heavy ion irradiation without DNA damage.[3] Approximately 27 insect species can survive in extreme conditions, such as extremely acidic environments (pH < 3).[4] From a material point of view, protection against such extreme environments is a surprising phenomenon considering that cuticles consist purely of organic materials without any metallic components.

For the aforementioned reasons, the chemistry of insect sclerotization, known as tanning, is unique. The tanning processes are mediated by phenolic enediol-to-quinone oxidation followed by crosslinking with nearby biomacromolecules such as polysaccharides and proteins.[5] In nature, polyphenol oxidation is mediated by enzymes such as polyphenol oxidase, and a high level of oxygen is essential for enzyme activity. Recently, phenol oxidation and subsequent crosslinking were found to readily occur at air/water interfaces even without enzymes.[6–8] A mechanically robust, free-standing film was spontaneously formed by nonenzymatic crosslinking between phenolic compounds (*e.g.*, dopamine or pyrogallol) and polyamines at the air/water interface. In an interfacial oxygen-rich layer, oxygen

[a] *Department of Chemistry, KAIST, Daejeon 34141, South Korea. E-mail: haeshin@kaist.ac.kr*
[b] *Department of Emerging Materials Science, DGIST, Daegu 42988, South Korea. E-mail: seonkihong@dgist.ac.kr*

† Electronic supplementary information (ESI) available. See DOI: 10.1039/c9mh01448a

reduction and phenol oxidation are coupled. Then, the oxidized phenol-quinone reacts with polyamines,[9] which form phenol-amine films at the air/water interface. This occurrence might explain why nature places a fully hardening organic material as the outer layer of insects (*i.e.*, exoskeleton), because it is directly exposed to air. Similar phenolic air/water interface chemistry also occurs in fruits. Fruit browning is the process of forming a brown-colored interfacial layer when internal polyphenol components in fruits are exposed to air,[10] as shown in the schematic of Fig. 1a. This reaction is also catalyzed by polyphenol oxidases when activated by the oxygen molecules provided by contact with air at the interface,[11,12] a property which is utilized by insects to heal their open wounds,[13,14] and thus does not occur in a vacuum. Fruit polyphenols containing catechol (R = –H) in Fig. 1b and pyrogallol (R = –OH) functional groups are oxidized to their corresponding quinone forms by air exposure.

We hypothesized that we could utilize the air/water interfacial chemistry inspired by insect cuticle formation to form a durable, protective organic armor layer against extreme environmental stimuli. Some cuticles are known to provide such protective

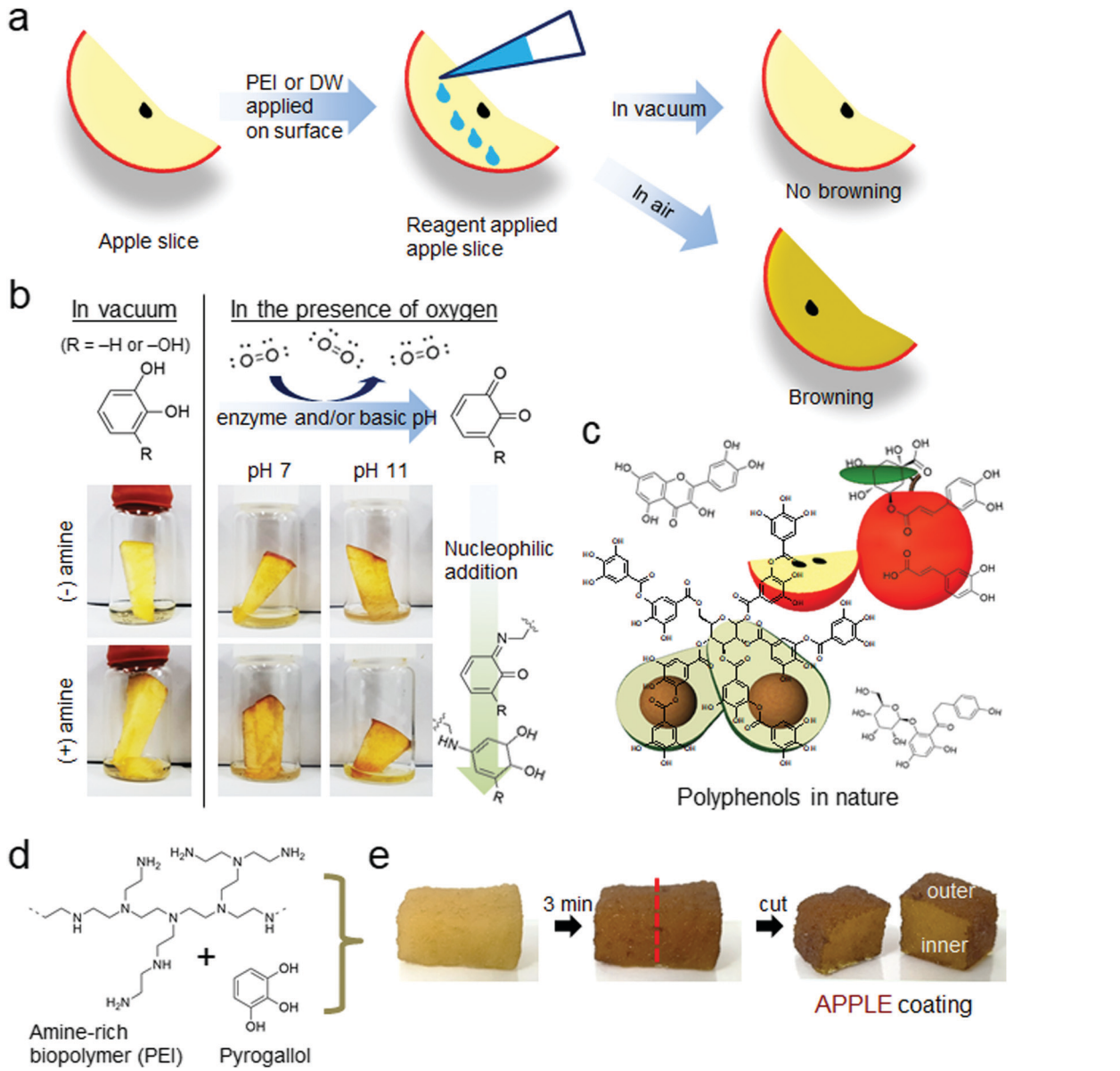

Fig. 1 APPLE coating formation. (a) Schematic of the fruit browning test. (b) Monitoring of fruit browning in various conditions explains the chemical mechanism of forming the APPLE coating. Oxygen turns on both enzymatic and pH-induced catechol (R = H) and gallol (R = OH) oxidation followed by crosslinking with surrounding biopolymers, which is the so-called fruit browning process. (c) Examples of various polyphenols found in nature, which were mimicked to find (d) the chemical component of the APPLE coating: an amine-rich polymer, polyethyleneimine (PEI), and pyrogallol (PG), which is one of the abundant substructures of polyphenols in plants, are simply dissolved in water followed by application to the surface of materials. (e) Demonstration of the APPLE coating formation on the surface of a sponge. After 3 minutes from the absorption of the coating solution, a dark-brown, thin-layered APPLE coating is formed at the outer edge, which is exposed to air, leaving the inner parts unchanged.

effects and enable organisms to survive under extreme environments.[15] Tardigrades, with their outer layer composed of cuticles, are known for their extreme survivability and have been recently reported to withstand vacuum space without dying.[16–18] A species of insect tick, *Haemaphysalis flava*, was also shown to survive under short term exposure to a vacuum environment and retain water in its body.[19] Therefore a high vacuum condition, such as that in an electron microscopy (EM) chamber, was chosen to be an extreme environment for this study. We expected the coating to protect soft materials from dehydration, followed by shrinkage under high vacuum, and act as a thermal insulator preventing melting/deformation of the low-temperature-melting soft materials. Both properties can be used for a thin organic coating useful for scanning electron microscopy (SEM) imaging. We named the nature-inspired protective coating "aerobic oxidation of polyphenol leading to artificial exoskeleton" (APPLE), and this coating layer is formed at the air/solid interface catalyzed by gaseous oxygen. Soft material SEM imaging suffers from (1) rapid dehydration *via* emitting vapor gas molecules and (2) mandatory metal depositions modifying the original surface morphology. Thus, the APPLE coating described herein is the first method to form a metal-free polymeric layer suitable for high-vacuum SEM chamber conditions exhibiting enhanced image resolution.

Results

APPLE coating

Before introducing the APPLE coating, a simple test was conducted to show the importance of oxygen in phenolic browning oxidation using a slice of apple. Fig. 1b shows that browning does not occur in a vacuum even though polyphenol oxidase exists within the apple slice. In the presence of air, however, a brown color was detected in the air-exposed areas of the apple slice even after being washed with water at pH 11. The strong alkaline pH inactivates most enzyme activities. The browning at pH 11 is consistent with previous studies[6–8] on polyphenol crosslinking at air/water interfaces without the addition of enzymes. Further addition of poly(ethylenimine) (PEI), an amine-rich polymer, produces darker browning possibly due to reactions between the quinones and the amine groups of PEI.

The APPLE coating at the interface is a result of a spontaneous reaction. The APPLE coating solution is composed of simply two components: (1) pyrogallol, the simplest form of many polyphenol derivatives that is abundantly found in plants, as shown in Fig. 1c, and (2) a polyamine, PEI (Fig. 1d). Simple absorption of this solution on a sponge resulted in the generation of an interfacial film covering the outer layer of a sponge exposed to air, which displayed a dark brown color similar to fruit browning without enzymes (Fig. 1e). The thickness of this film is highly dependent on the exposure time of oxygen in ambient air, and the detailed film formation mechanism was previously report by Wang *et al.* They observed that a free-standing film was generated at the air/water interface for an aqueous solution containing PEI and PG. By thirty-minute exposure of the solution to air, a 5 μm film thickness was observed with no further growth of the film even after long-term air exposure.[7] This study indicates that the naturally formed oxygen-rich layer created at the air/water interface plays an important role in the formation of the film. Therefore, various methods such as centrifugal filtration and spin coating methods have been optimized to minimize the air exposure time down to a few minutes to make the thickness of the coating thin. It was found that this coating protects soft materials from dehydration and shrinkage under high vacuum conditions and acts as a thermal insulator preventing melting/deformation of polymeric materials under electron beam irradiation.

Biological wet substrates require several sample preparation steps prior to imaging through scanning electron microscopy (SEM) to prevent structural collapse and deformation by dehydration under high vacuum (10^{-5}–10^{-6} Torr) during imaging. The conventional method of wet sample preparation for SEM imaging is described in a scheme in Fig. 2a. A fixation step involves maintaining the wet sample shape through various chemical treatments, such as formaldehyde treatment for tissue samples. Then, the dehydration step removes water from the fixed sample, usually by multiple washings with gradually increasing concentrations of ethanol. The dehydrated, fragile (due to the absence of water) sample needs to be dried by a critical point drying process. The sample preparation usually takes several hours to days, and is a time-consuming and labor-intensive process. Metal sputtering prior to imaging is also mandatory for nearly all organic substrates due to the electrons built up on insulating organic surfaces. Often, uncontrolled discharge in organic samples leads to failure in obtaining SEM images.

The APPLE reaction allows single-step, surface protective coating generation on organic wet substrates so that they can survive against dehydration followed by deformation in a vacuum. Therefore, one can replace the laborious steps, including fixation, dehydration, critical point drying and metal sputtering, with one single APPLE coating step, which takes less than 5 minutes. Several different methods of applying the APPLE coating were conceived, depending on the shapes and sizes of the wet substrates that needed to be imaged. While simple dip coating of a sample was sufficient for relatively large structurally intact samples, very small or very flexible (and therefore hard to handle) samples needed to be coated with different methods. For small, microsized beads and particular samples, the coating was applied with a filtered centrifuge, as seen in Fig. 2b(i), where poly(methyl methacrylate) (PMMA) microbeads were coated with the APPLE solution by placing the beads in filtration tubes with polyethylene frits placed inside. Then, the PEI/PG solution was placed in the tubes and centrifuged, which resulted in coated beads on the frits, which were separated from the solution by the frit. To verify the successful application of APPLE on the beads with this method, the zeta potentials of APPLE-treated beads and bare beads were compared. The zeta potential was determined to be −22.7 mV (n = 3) for the bare beads, while it was +18.7 mV (n = 3) for the APPLE-treated

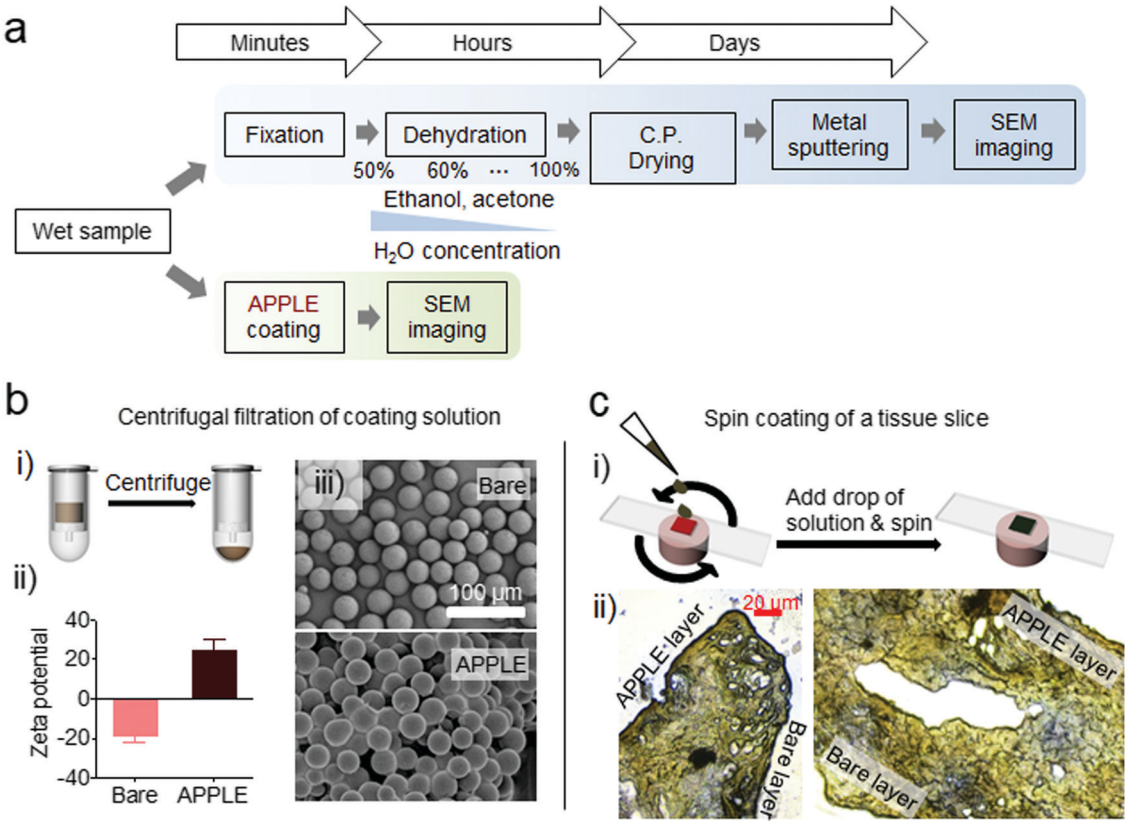

Fig. 2 APPLE coating method optimization. (a) Schematic comparison of conventional labor-intensive sample preparation steps of biological samples for SEM analysis and a single-step APPLE coating. (b) The APPLE coating method for microbeads: (i) schematic of the APPLE coating process by utilizing centrifugal filtration (4000 rpm for 1 min, pore size of membrane filter: 30 μm), (ii) surface charge conversion after APPLE coating measured by zeta potential (n = 3), and (iii) SEM images of coated and bare microbeads indicating that a nanothin APPLE coating is generated on the surface not affecting the entire size of the beads. (c) The APPLE coating method optimized for a tissue slice: (i) schematic of APPLE coating applied by spin-coating (5000 rpm for 0.5 min), and (ii) microscope image of sectioned, single-side APPLE spin-coated porcine liver.

beads, confirming the incorporation of positively charged protonated PEI on the surface of the beads (Fig. 2b(ii)). Further characterization of the surface morphology of these beads was performed as shown in Fig. 2b(iii), and no shape or size difference between the bare and APPLE-treated beads was observed, indicating that the APPLE coating is sufficiently thin on the nanometer scale. For soft samples that cannot be dip coated without complications due to their high flexibility, the samples were spin coated on top of a solid support, as seen in Fig. 2c(i). There was no visible thickness difference between the coated and uncoated sides of the sample, which confirms the thin nature of the APPLE spin coating. Microscopic analysis also exhibited no apparent differences between the two layers, as shown from the microscopic image for the microtome-sectioned slices of APPLE-coated porcine liver in Fig. 2c(ii). Statistical analysis (Fig. S1, ESI†) confirmed that the diameters of the APPLE-treated and bare microbeads in Fig. 2b(iii) were not significantly different (APPLE-treated beads: 32.534 ± 2.328 μm, bare beads: 32.248 ± 1.859 μm, p = 0.6335), and the thicknesses of the edge shown in the microscopic images of the APPLE edge and bare edge in Fig. 2c(ii) were also similar (APPLE edge: 1.578 ± 0.220 μm, bare edge: 1.742 ± 0.402 μm, p = 0.0811).

The chemical composition of APPLE was analyzed by various spectroscopic tools. The spectrum obtained by X-ray photoelectron spectroscopy (XPS) showed the co-existence of nitrogen (N1s, ~399 eV) and oxygen (O1s, ~531 eV) on APPLE (Fig. S2, ESI†). The intensity of the silicon 2p peak was very small, indicating that the thickness of the APPLE coating on the silicon wafer is on the order of 10–15 nm, the typical depth limitation in XPS. As for the carbon (C1s), there were peaks attributed to C–C (~284.8 eV) from both PEI and PG. Additionally, the C–O and C–N peaks (~285.5 eV) were attributed to PG and PEI, respectively. There was also a small peak that appeared at ~287.5 eV, which was attributed to C═O from the oxidized PG. Infrared spectroscopy showed various functional groups in APPLE; a peak detected at 1690–1650 cm^{-1} indicates C═N and/or C═O groups, a broad peak at 3500–3300 cm^{-1} indicates the presence of –OH, –NH and $-NH_2$ groups, and a doublet peak at 2950–2750 cm^{-1} possibly indicates the aldehyde –CH. The peaks detected at 1560 cm^{-1} (cyclic alkene) and 1390–1350 cm^{-1} (phenol) indicate the presence of PG in the film, while the peak at around 1465 cm^{-1} might represent –CH (alkane) from the PEI chains. The characteristic peak at 1320–1290 cm^{-1} represents C–N from aromatic amines (crosslinked PEI and PG), which suggests covalent crosslinking between PEI

and PG (Fig. S3, ESI†). Additionally, the air-induced oxidization following heterogeneous oligomerization/polymerization of PG was investigated by monitoring a broad absorbance range from ultraviolet to visible using a UV/vis spectrophotometer (Fig. S4, ESI†). Finally, the bulk APPLE contained about 20% water to total weight that mostly escaped at around 90–100 °C, and the dehydrated APPLE was completely degraded at around 300–400 °C, confirmed by both thermal gravimetric analysis (TGA) and differential scanning calorimetry (DSC) (Fig. S5, ESI†).

Dehydration prevention and structural support

The dehydration protection performance of the APPLE coating was tested with a model soft wet sample, a hydrogel. A 1% agarose hydrogel was dip-coated *via* the APPLE reaction and then placed on top of a membrane filter, the bottom of which was connected to a vacuum pump, as shown in Fig. 3a. The resulting change in height of the APPLE-coated gel and the bare gel is seen in Fig. 3b. The bare gel lost approximately one-third of its height over 8 minutes in a weak vacuum, whereas the APPLE-coated gel withstood major shrinkage over 8 minutes in a vacuum (n = 5). Dehydration was reflected by the loss of conductance of both gels, as seen in Fig. 3c, where the bare gel lost most of its conductance after 3 hours in a vacuum, while the APPLE-treated gel mostly retained its conductance (n = 10).

This protective effect of APPLE on the gel was confirmed using high vacuum (10^{-5}–10^{-6} Torr) and SEM. The APPLE-treated gel and the bare gel were placed together on top of a sample holder ('before' image of Fig. 3d) for SEM imaging.

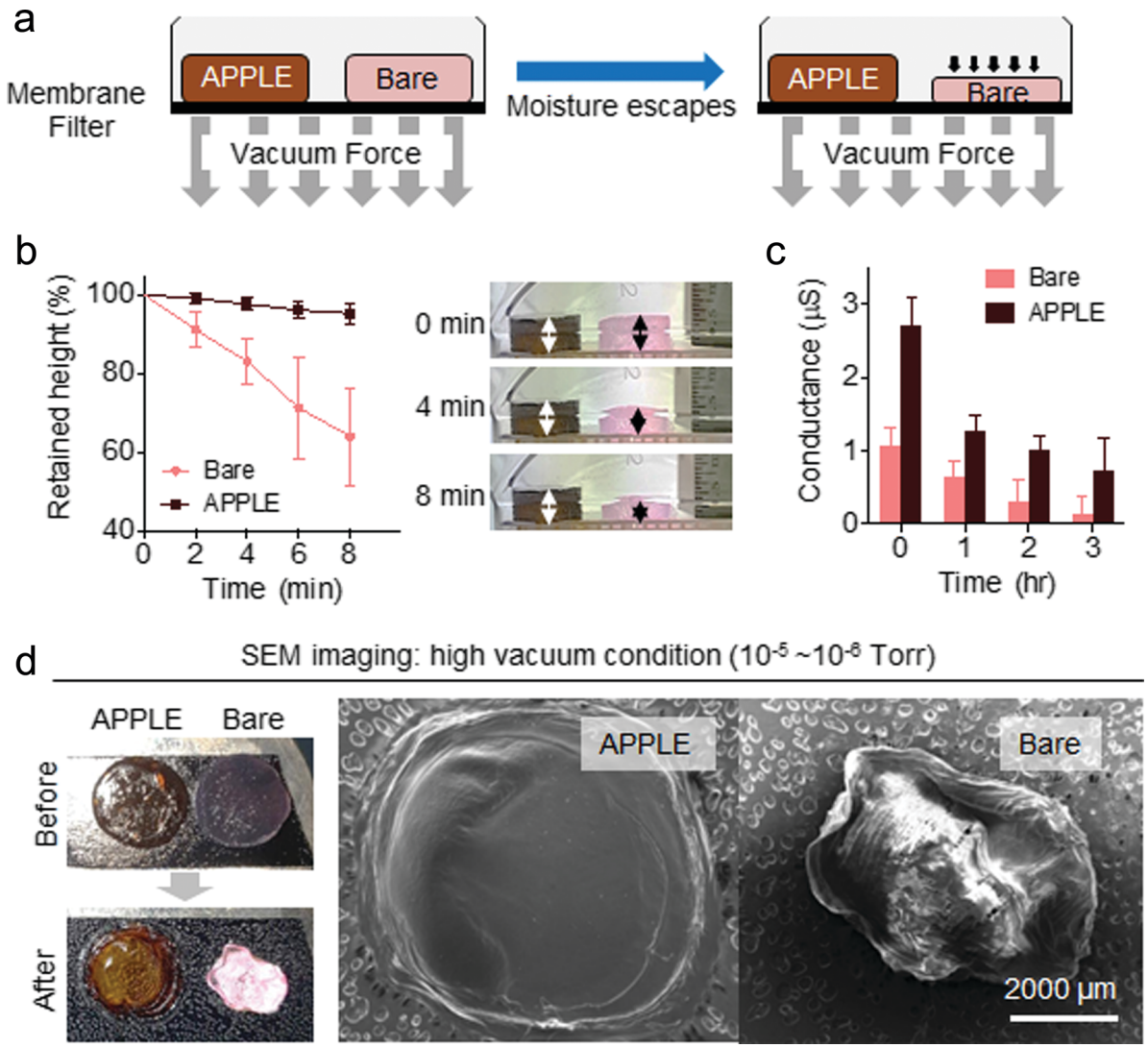

Fig. 3 Dehydration protection capability of APPLE under vacuum pressure. (a and b) Experimental design and the results on the shrinkage prevention effect of the APPLE coating applied on the surface of a hydrogel (n = 5). No shrinkage was observed on the APPLE-coated hydrogel (brown color). (c) Conductance change of the APPLE-coated and bare agarose hydrogel stored under vacuum over 3 hours (n = 10). (d) SEM imaging of APPLE-coated hydrogels performed under high vacuum (10^{-5}–10^{-6} Torr) without metal sputtering as well as the conventional dehydration process. Note that no charging effect was observed on the APPLE-coated hydrogel, which remains hydrated under vacuum (left). Uncoated hydrogels were deformed, and charging occurred due to rapid dehydration (right).

As seen in the 'after' image of Fig. 3d, only the APPLE-treated gel was able to retain its original shape, with minor visible water loss. In comparison, the bare gel lost most of its water content and became opaque, resulting in complete collapse of its original shape after SEM imaging under high vacuum. In the SEM images in Fig. 3d, one interesting thing to note is that the bare gel seems to display high charge in its image, whereas the APPLE gel was uncharged. Neither sample was metal sputtered. This difference might be because the APPLE-treated gel still retained water inside of the gel during imaging and thus had minor conductivity on the surface, resulting in less charge in the resulting image. In addition to the SEM chamber under vacuum, the dehydration protection capability of APPLE was also tested under 100% humidity, in air at room temperature, and in a 60 °C oven. As seen in Fig. S6 (ESI†), the APPLE-coated gels were found to be better able to resist dehydration compared to the uncoated bare gels. In a 100% humidity chamber, both gels experienced no dehydration. Recent studies have reported similar surface treatment approaches by skipping the metal sputtering steps in SEM imaging.[20–24] Several different methods, such as a plasma nitride layer, an osmium–thiocarbohydrazide–osmium layer, and ionic liquids, have been suggested as alternatives for sputter coating; however, ionic liquid and osmium–thiocarbohydrazide–osmium methods are more akin to shape preservation methods and thus require sample drying steps, and plasma nitrating can only be utilized for hard materials such as metals.

Thermal shield properties

In addition to its dehydration prevention and shape protection, the APPLE coating can also act as a thermal insulator protecting inner polymeric substrates against melting/deformation, as shown in Fig. 4a. The thermal conductivity of the APPLE film was measured to be 0.329 W m^{-1} K^{-1} (n = 5), which is on par with the thermal conductivity of conventional epoxy, 0.334 W m^{-1} K^{-1} (Fig. 4b).[25] The crosslinking of pyrogallols during APPLE formation

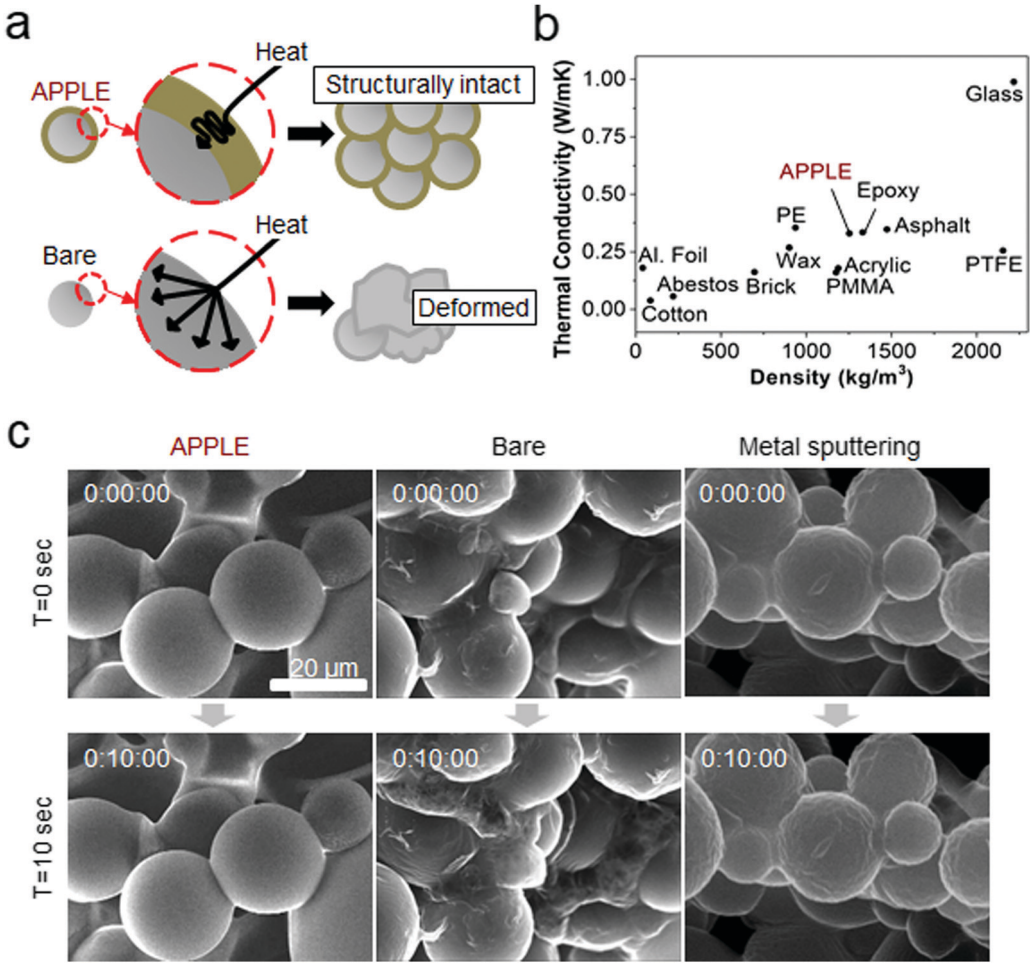

Fig. 4 APPLE coating as a thermal insulator. (a) Schematic proposal of the APPLE coating as a thermal insulating layer to prevent melting of nano/microsized polymeric materials under an electron beam during SEM imaging. (b) Comparison of the thermal conductivity of various commonly used thermal insulators and APPLE coatings (n = 5 for APPLE). (c) Video caption images of APPLE-covered, uncoated polycaprolactone (PCL) microbeads and a positive control prepared by conventional metal sputtering. Due to the low melting point (~60 °C), uncoated PCL rapidly melted under the electron beam even before recording (middle), and the metal-coated particles also started to show wrinkles on the surface (right), whereas the APPLE-covered particles remained without deformation by thermal protection from the APPLE coating (left).

results in polyphenol-like chemical structures similar to those found abundantly in plants, which are used for various protective roles, for example as antioxidants. Abundant polyphenol crosslinking with polymers has been shown to increase mechanical strength and previous studies have shown that incorporating tannic acid into a polymer generally results in increased mechanical properties in the polymer.[26] Tannins especially have been shown to have thermal protective abilities[27,28] and thermal protective properties similar to those of other common insulators can be achieved. Frequent problems in SEM imaging of polymeric materials even after metal sputtering are not only due to dehydration but also melting by the high-energy electron beam (0.2 to 40 keV). We hypothesized that the melting of polymeric materials such as polycaprolactone (PCL) can be inhibited by the APPLE coating, which possesses thermal protective abilities. When placed in the SEM chamber, the APPLE-coated PCL beads were able to maintain their shape without deformation, while the bare beads lost their structure and melted together into large clumps in the SEM chamber over several seconds (Fig. 4c and Videos S1–S3 in the ESI†). After thin metal sputtering, the beads

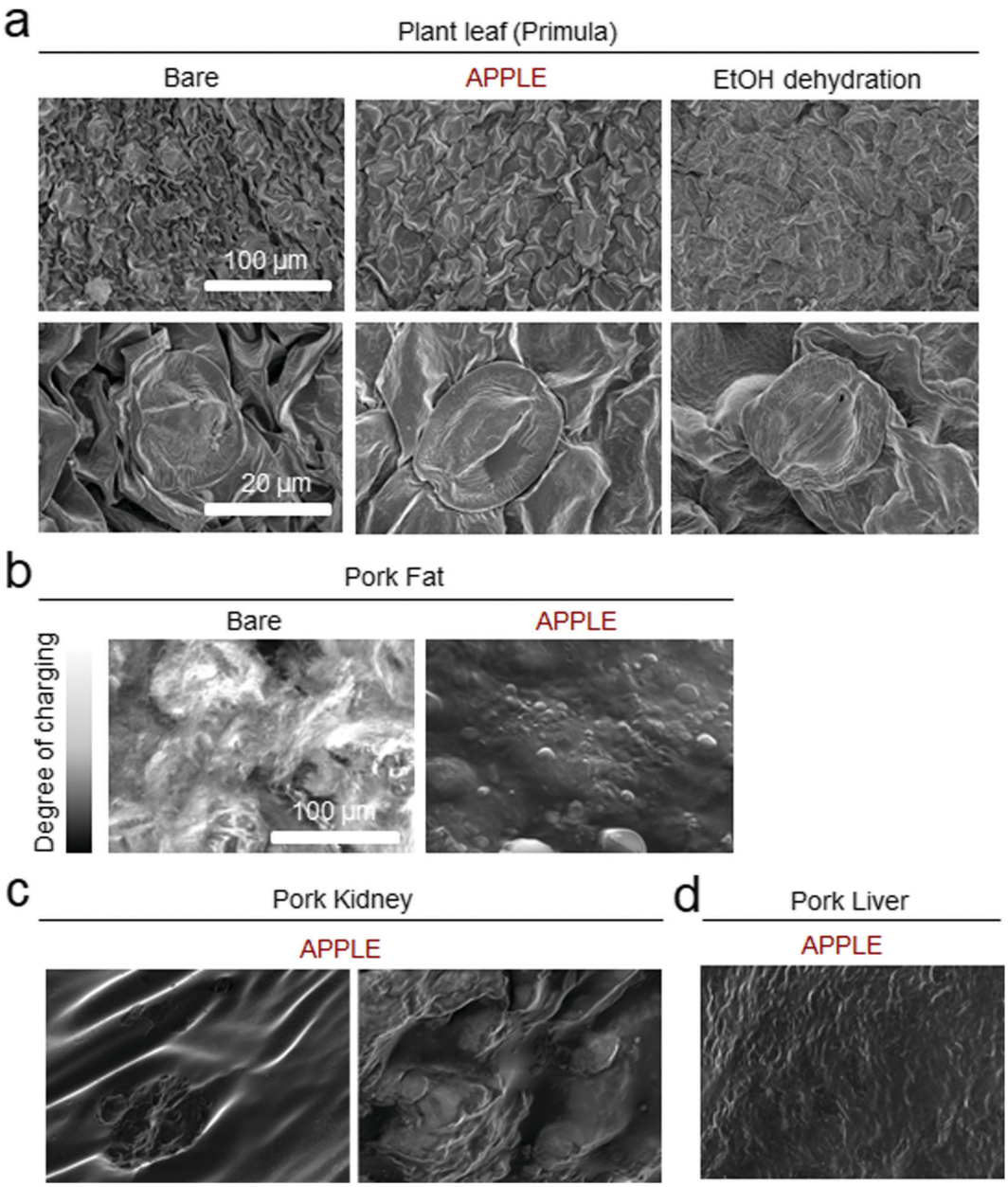

Fig. 5 SEM images of various biological tissues prepared by the APPLE method. (a) SEM images of a plant leaf of a flower, Primula, showing the stomata without shrinkage after APPLE coating treatment. (b) SEM images of porcine fat showing dramatic attenuation of the charging effect after APPLE coating treatment by dehydration protection of wet tissue. Porcine kidney (c) and liver (d) could also be prepared by APPLE coating for SEM imaging. All samples were not treated by metal sputtering except for the ethanol dehydrated plant leaf due to the intrinsic absence of water on the wax layer of the leaf producing a charging effect even after APPLE coating treatment.

were able to withstand deformation better than the non-sputtered ones; however, the surface of the beads wrinkled over several seconds due to melting of the inner polymers under the metal layer, which is a well-known heat generator under energy irradiation.

Wet tissue imaging applications

Finally, various biological wet substrates could be imaged through SEM using the APPLE coating technique. A piece of plant leaf (Primula) was prepared *via* the APPLE method, a conventional dehydration/drying process, and without any treatment as a negative control, and then imaged by SEM without metal sputtering (Fig. 5a). Even with the intrinsic low water content and the existence of a dehydration-protective wax layer of the leaf,[29] the microstructure of the completely bare leaf collapsed, resulting in a highly wrinkled surface morphology. The leaf that was conventionally processed *via* dehydration with a gradient concentration of ethanol resulted in a relatively flat looking leaf surface, possibly due to the dissolution of the wax layer in ethanol. The APPLE-treated leaves showed superior 'plumpness' relative to the bare counterpart, and most of the surface structure seemed to be firm. In Fig. 5b, the effect of the APPLE coating on a piece of porcine fat in an SEM image can be seen. The bare porcine fat image is nearly unintelligible due to charging, but a thin layer of the APPLE coating seems to be able to prevent a large degree of charging and results in a relatively clean image with distinguishable fat molecules. In addition, the APPLE coating was also successfully applied to three-dimensional native organs by dip coating; a cubic shaped slice of porcine kidney and liver were imaged as model substrates, as shown in Fig. 5c and d. Both images could be observed without any charge, and furthermore, the image could be zoomed in without complications to display the characteristic contours of the biological tissue surface, which can be credited to the thin coating from spin coating.

Conclusions

In conclusion, we have developed a fruit browning mimetic protective coating providing dehydration, shrinkage, and thermal protective properties *via* the APPLE reaction for wet samples to be used in high vacuum environments such as SEM imaging. The APPLE coating was applied to samples with varying methods, such as simple dip-coating, centrifugal filtering, and conventional spin-coating processes. A single step, 5 minutes process of the APPLE coating allows SEM imaging of APPLE-treated soft wet samples without the conventional laborious steps of fixation, dehydration, drying, and metal sputtering. In addition, the APPLE-treated samples displayed less charge in the acquired SEM images, possibly due to retaining surface moisture and providing conductivity for imaging. Our findings for this novel protective coating for SEM analysis will be useful for simplifying future wet sample SEM imaging protocols.

Experimental methods

APPLE preparation

The coating solution was prepared by mixing aqueous solutions of 20 wt% polyethyleneimine (PEI) (Sigma-Aldrich, M_W = 750 000) and 0.2 M pyrogallol (PG) (Sigma-Aldrich) at a 1 : 1 volume ratio. APPLE formation was performed using centrifugal filters for microbeads, the conventional spin-coating method for sliced tissues, and spin coating for three-dimensional substrates. In detail, approximately 20 mg of poly(methyl methacrylate) microbeads (PMMA, from Cospheric, 27–32 μm in diameter) or polycaprolactone microbeads (PCL, from Phosphorex, ~20 μm in diameter) was placed in a centrifugal filter (Supelco, polyethylene frit, 20 μm porosity), and the APPLE solution was centrifuged through the column at 5000 rpm for 1 minute. The beads were then washed once with distilled water and dried by centrifugation under the same conditions. For sliced biological samples, 30 μL of the APPLE solution was quickly dropped on top of the 0.5 cm × 0.5 cm sized sample, spinning at 5000 rpm for 15 seconds on a spin coater (ACE-200, Dong Ah Trade Corp). Three-dimensional samples, such as hydrogels, were directly immersed into the APPLE solution and then removed after 1–2 seconds. The excess solution on the surface of the samples was immediately wiped off with a paper towel or simply shaken out.

Fruit browning test. An apple (purchased from the local supermarket) was cut into pieces small enough to fit inside a 20 mL glass vial. For vacuum tests, the glass vials were sealed with a rubber stopper after placing a piece of apple inside. Then, the air inside was vacuumed with a vacuum hose with a needle attached to one end, which was used to pierce the rubber stopper to access the vial. One milliliter of distilled water was added by syringe inside the negative-amine test, while 1 mL of PEI 20 wt% solution (pH = 11) was added by syringe into the positive-amine test. For the various pH conditions in the air, distilled water or the PEI solution with adjusted pH (7 or 11) was added by adding 1 M hydrogen chloride (for PEI) or sodium hydroxide (for distilled water) and applying it to the surfaces of the sliced apple pieces.

Microbead characterization

The zeta potential of the APPLE-treated PMMA microbeads dispersed in distilled water was measured with a Zetasizer nanoseries (MAL1160456, Malvern) to confirm the positively charged APPLE formation on the surface of the negatively charged PMMA microbeads. The surface morphology of the APPLE-treated PMMA beads and the heat resistance of the APPLE-treated PCL beads were obtained using ultrahigh-resolution cold field emission SEM (SEM SU8230, Hitachi) with an accelerating voltage of 1.6 kV. The bare sputter-coated beads were coated with platinum sputter coating for approximately 30 seconds.

Shape and conductance changes of the hydrogels in a vacuum

Agarose gel was prepared by dissolving 1% agarose (Bioneer) in boiling water followed by cooling down to room temperature.

The gel was cut to a fixed size of 0.5 cm in height and 1 cm in diameter for the shrinkage test. One of the gels was dip coated with APPLE solution using the method mentioned above, while the other gel was treated with distilled water as a negative control. The gels were then placed on top of a lidless membrane filter (Corning, 0.22 μm pore, cellulose acetate), the bottom of which was connected to a vacuum pump, and changes in the height of the gels were recorded over time. In addition, the decrease in conductance was monitored as the gels were dehydrated under vacuum. APPLE-treated and bare agarose gels were placed in an enclosed vacuum chamber (gauge pressure = −0.08 MPa) over 3 hours, and the resistivity of the gels was measured using a digital multimeter (Hontek, A830L) with the prongs touching the edges of the gels keeping them 1 cm apart from each other. Then, the conductance was calculated to be 1/the measured resistance. The surface morphology of the APPLE-treated gel was obtained using a field emission microscope (Magellan 400, FEI Company) with an accelerating voltage of 5 kV.

Heat conductivity

The APPLE solution was thinly spread on top of a Petri dish and cured at room temperature over 48 hours. The cured APPLE layer was gently peeled from the Petri dish using tweezers, and the heat conductivity of the film was measured using a heat flow meter (HFM 436 Lambda, Netzsch) without a solid support. The heat conductivity of the various substrates was referenced from previous studies.[25]

Native wet tissue imaging

A plant leaf of the Primula flower, porcine kidney, porcine liver, and fat from thinly sliced porcine belly meat (purchased from the local supermarket) were cut into squares with a fixed size of 1 cm by 1 cm. The leaf and various porcine parts were then placed on a glass slide and spin coated with the methods mentioned above and imaged with ultrahigh-resolution cold field emission (SEM SU8230, Hitachi) and field emission microscopy (Magellan 400, FEI Company), with additional porcine tissues being sectioned at a thickness of 10 μm using a cryo-microtome (Leica CM3050 S, Leica Biosystems) and imaged by a fluorescence microscope (Eclipse 80i, Nikon).

Conflicts of interest

The authors declare no conflict of interest.

Acknowledgements

The authors would like to thank Mrs Ji Youn Park at CCRF for sharing her expertise in SEM analysis. This research was supported by National Research Foundation of Korea (NRF) grants funded by the Government of Korea (MSIT): Basic Science Research Program (NRF-2018R1D1A1B07045249 to S. H.), Convergence R&D over Traditional Culture and Current Technology (NRF-2016M3C1B5906485 to H. L.), and Center for Multiscale Chiral Architectures, Science Research Center (SRC) Program (2018R1A5A1025208 to H. L.). This work was also carried out with the support of the Cooperative Research Program for Agriculture Science and Technology Development (Project PJ01323201 to S. H.) from the Rural Development Administration of the Republic of Korea.

References

1 H. E. Hinton, *Nature*, 1960, **188**, 336.
2 M. Watanabe, T. Kikawada, N. Minagawa, F. Yukuhiro and T. Okuda, *J. Exp. Biol.*, 2002, **205**, 2799.
3 O. Gusev, Y. Nakahara, V. Vanyagina, L. Malutina, R. Cornette, T. Sakashita, N. Hamada, T. Kikawada, Y. Kobayashi and T. Okuda, *PLoS One*, 2010, **5**, e14008.
4 G. G. Rodrigues and B. W. Scharf, *Mine Water Environ.*, 2001, **20**, 114.
5 J. H. Waite, *Methods Enzymol.*, 1995, **258**, 1.
6 S. Hong, C. F. Schaber, K. Dening, E. Appel, S. N. Gorb and H. Lee, *Adv. Mater.*, 2014, **26**, 7581.
7 Y. Wang, J. P. Park, S. H. Hong and H. Lee, *Adv. Mater.*, 2016, **28**, 9961.
8 F. Ponzio, P. Payamyar, A. Schneider, M. Winterhalter, J. Bour, F. Addiego, M.-P. Krafft, J. Hemmerle and V. Ball, *J. Phys. Chem. Lett.*, 2014, **5**, 3436.
9 H. Lee, S. M. Dellatore, W. M. Miller and P. B. Messersmith, *Science*, 2007, **318**, 426.
10 T. M. Reynolds, *Adv. Food Res.*, 1963, **12**, 1.
11 M. Ashida and P. T. Brey, *Proc. Natl. Acad. Sci. U. S. A.*, 1995, **92**, 10698.
12 K. Robards, P. D. Prenzler, G. Tucker, P. Swatsitang and W. Glover, *Food Chem.*, 1999, **66**, 401.
13 K. D. Clark and M. R. Strand, *J. Biol. Chem.*, 2013, **288**, 14476.
14 R. P. Sorrentino, C. N. Small and S. Govind, *Biotechniques*, 2002, **32**, 815.
15 J. C. Wright, *Tissue Cell*, 1989, **21**, 263.
16 D. Persson, K. A. Halberg, A. Jorgensen, C. Ricci, N. Mobjerg and R. M. Kristensen, *J. Zool. Syst. Evol. Res.*, 2011, **49**, 90.
17 N. Mobjerg, K. A. Halberg, A. Jorgensen, D. Persson, M. Bjorn, H. Ramlov and R. M. Kristensen, *Acta Phys.*, 2011, **202**, 409.
18 K. I. Jonsson, E. Rabbow, R. O. Schill, M. Harms-Ringdahl and P. Rettberg, *Curr. Biol.*, 2008, **18**, R729.
19 Y. Ishigaki, Y. Nakamura, Y. Oikawa, Y. Yano, S. Kuwabata, H. Nakagawa, N. Tomosugi and T. Takegami, *PLoS One*, 2012, **7**, e32676.
20 S. V. Buravkov, V. P. Chernikov and L. B. Buravkova, *Bull. Exp. Biol. Med.*, 2011, **151**, 356.
21 K. Kawai, K. Kaneko, H. Kawakami and T. Yonezawa, *Langmuir*, 2011, **27**, 9671.
22 K. Horigome, T. Ueki and D. Suzuki, *Polym. J.*, 2016, **48**, 273.
23 A. Varesano, B. Antognozzi and C. Tonin, *Synth. Met.*, 2010, **160**, 1683.
24 O. Öztürk, S. Okur and J. P. Riviere, *Nucl. Instrum. Methods Phys. Res., Sect. B*, 2009, **267**, 1540.
25 R. R. Zarr, J. A. Chavez, A. Y. Lee, G. Dalton and S. L. Young, NIST Standard Reference Database Number 81: NIST Heat

Transmission Properties of Insulating and Building Materials, National Institute of Standards and Technology, https://srdata.nist.gov/insulation/, Retrieved 2019.
26 A.-S. Hager, K. J. R. Vallons and E. K. Arendt, *J. Agric. Food Chem.*, 2012, **60**, 6157.
27 H. A. Shnawa, Y. Jahani, M. N. Khalaf and A. A. H. Taobi, *Open J. Org. Polym. Mater.*, 2015, **5**, 69.
28 M. C. Basso, X. Li, V. Fierro, A. Pizzi, S. Giovando and A. Celzard, *Adv. Mater. Lett.*, 2011, **2**, 378.
29 C. Buschhaus and R. Jetter, *Plant Physiol.*, 2012, **160**, 1120.

